Diffusion tensor imaging revealed different pathological processes of white matter hyperintensities

Zhigang Min
The Affiliated Yixing Hospital of Jiangsu University
Hairong Shan
The Affiliated Yixing Hospital of Jiangsu University
Long Xu
The Affiliated Yixing Hospital of Jiangsu University
Daihai Yuan
The Affiliated Yixing Hospital of Jiangsu University
Xuexia Sheng
The Affiliated Yixing Hospital of Jiangsu University
Wenchao Xie
The Affiliated Yixing Hospital of Jiangsu Universi
Zhi-hong Cao (profczh@gmail.com)
The Affiliated Yixing Hospital of Jiangsu University https://orcid.org/0000-0002-4354-2139

Research article

Keywords: White matter hyperintensities; diffusion tensor imaging; pathological processes

Posted Date: August 14th, 2019

DOI: https://doi.org/10.21203/rs.2.12723/v1

Abstract

Background The purpose of this study was to verify the pathological heterogeneity of white matter hyperintensities (WMHs). We compared diffusion tensor imaging (DTI) metrics within different brain regions using identical grading protocols, and subsequently investigated the microstructural changes in these areas as the WMH progressed. Methods Seventy-three patients with WMH and 18 healthy controls who received DTI were included in this study. We measured fractional anisotropy (FA), mean diffusivity (MD), axial diffusivity (DA), and radial diffusivity (DR) of periventricular and deep WMH in six brain regions and grouped these measures according to the Fazekas scale. We then compared the DTI metrics of different regions with the same Fazekas scale grade. Results Significantly lower FA values (all $p<0.001$), and higher MD (all $p<0.001$) and DR values (all $p<0.001$) were associated with WMH observed within the periventricular white matter around the frontal horn (pFH) and the frontal lateral ventricle (pFLV) compared to other regions with the same Fazekas grades. However, in the normal white matter of the pFH and pFLV, FA was not significantly lower than all other regions. Furthermore, in these areas, MD, DA, and DR were not significantly higher than in all other regions. Conclusion Distinct pathological processes occurred within frontal periventricular WMH and other regions; these processes may represent the effects of severe demyelination within the frontal periventricular white matter.

Background

White matter hyperintensities (WMHs), which appear as hyperintense areas on T2-weighted imaging (T2WI) or fluid-attenuated inversion recovery (FLAIR) images, are common findings on magnetic resonance imaging (MRI). Existing evidence shows WMH severity is associated with the risk of dementia in the general population [1]. The two most commonly-used methods for evaluating WMH severity are qualitative grading scales and quantitative WMH volumetric measurements [2, 3]. However, correlations between WMH volume and cognitive performance are modest, and many clinical variations cannot be explained by volumetric measures [4].

Recent research showed that lesion location might be another important factor affecting cognition [5]. In the frontal lobe, parieto-occipital lobe, and other parts of the brain, periventricular WMHs are involved in cognitive function [4-7]. Carnevale et al. [5] found that alterations in specific white matter fiber-tracts were related to impaired cognition. Abnormal anterior thalamic radiation appears related to impaired memory, and the forceps minor seems to be involved in processing speed. Cremers et al. [8] suggested that the identification of tract-specific microstructural changes was helpful for understanding the mechanisms of cognitive impairment. Some studies have found that periventricular WMHs were significantly associated with various cognitive functions, while other studies showed that subcortical WMHs were involved; and a few other studies found no associations [9, 10]. Despite similar findings obtained using conventional MRI, WMHs exhibited heterogeneous pathologies. This might explain why some clinical variations cannot be determined by volumetric measures of WMH [11-13].

Habes et al. [14] supported the hypothesis that different underlying pathophysiologic mechanisms influenced regional patterns of WMH distribution; they found that frontal WMHs were more strongly associated with blood pressure and cortical atrophy, while only dorsal WMHs were associated with genetic risk factors for Alzheimer s disease. However, little is known about the pathological bases of these WMHs.

Diffusion tensor imaging (DTI) is a unique tool for identifying microstructural white matter changes and may be able to characterize pathological substrates of WMH since this technology can detect variations in microstructural integrity [15]. Studies using DTI and magnetization transfer imaging found a difference between frontal and parieto-occipital periventricular WMHs [16, 17].

We therefore hypothesized that WMHs that arose from different pathological processes would undergo different microstructural changes that could be detected by DTI. This study aimed to verify the pathological heterogeneity of WMHs by comparing DTI metrics, obtained from different brain regions, using the same grading scale. We additionally investigated microstructural changes in these brain regions.

Methods

Participants

Our institutional review board approved this study and written informed consent was acquired from each patient. We recruited males and females with WMHs, as confirmed by FLAIR or T2WI results. The Fazekas scale was adopted to classify periventricular and deep WMHs as grades 1, 2, or 3. All grades were calculated separately from areas within the frontal and parietal-occipital lobes. Two neuro-radiologists assessed each patient, and conflicting results were discussed until an agreement was reached. We additionally recruited adult males and females with normal white matter to serve as a control group.

DTI and Post-Processing

All patients and controls underwent DTI using a 3.0-T MR scanner (Philips Achieva, Best, the Netherlands) equipped with a 16-channel head-neck phased array coil. The imaging parameters were as follows: repetition time of 8000 ms, echo time of 87 ms, 32 directions, b-values of 0 and 1000 s/mm^2, a matrix of 112 × 112 interpolated to an image matrix of 224 × 224, and a slice thickness of 2 mm with no gaps. A total of 60 consecutive slices were acquired over 6 minutes. The raw data were exported to DTIStudio (Johns Hopkins University; https://www.mristudio.org/). Images were observed in "Original View" and excluded if there were motion artifacts. Using the Automated Image Registration (AIR) tool, we used an offine warp model to correct image distortions due to eddy currents and misregistration errors due to head motion. After data correction, fractional anisotropy (FA), mean diffusivity (MD), axial diffusivity (DA), and radial diffusivity (DR) maps were calculated.

Measurements

DTI metrics of periventricular and deep WMH were measured in six areas using one or two regions of interest (ROIs) consisting of approximately 12 voxels. These included the frontal, parietal, and occipital lobes. We determined that four periventricular ROIs were the most common locations of WHMs. These included areas around the frontal horn, occipital horn, frontal lobe, and parietal lobe of the lateral ventricle. The other two deep white matter lesion ROIs were located within the frontal and parietal centrum ovales. The six ROIs were as follows: periventricular white matter around the frontal horn (pFH), periventricular white matter around the frontal lateral ventricle (pFLV), periventricular white matter around the occipital horn (pOH), periventricular white matter around the parietal lateral ventricle (pPLV), deep white matter of the frontal centrum ovale (dFCO), and deep white matter of the parietal centrum ovale (dPCO). We used colored FA maps to confine the ROIs within identical white matter tract locations (Figure 1). Mean diffusion-weighted imaging maps were used to keep the cerebral spinal fluid outside the ROI. The average FA, DA, and DR values of periventricular WMHs and normal white matter were measured in the frontal, parietal and occipital lobes.

Statistical analysis

All statistical analyses were performed using SPSS software (version 22, IBM, Armonk, NY, USA), and two-sided p values <0.05 indicated a significant difference. Spearman correlation analysis was used to explore the relationship between DTI parameters and Fazekas scale scores. One-way analysis of variance (ANOVA) was used to identify

differences in FA, MD, DA, and RD values among different regions with the same Fazekas grade. The Tukey's test was used for comparing values.

Results

A total of 73 patients were recruited. All exhibited WMHs, as confirmed by FLAIR or T2WI results. There were 42 male and 31 female patients, with an average age of 72.6 years. Eighteen older people with normal white matter were recruited as a control group. Healthy controls included ten males and eight females with an average age of 65.4 years.

With increasing Fazekas grades, the DTI metrics of WMHs in different regions showed similar changes. FA values decreased, and MD, DA and DR values increased as the Fazekas grade increased (Figures 2–5). Spearman correlation analysis showed that FA, MD, DA, and DR values in all regions were significantly correlated (p<0.001) with Fazekas grades, with the exception of the WMH FA value in the pPLV (p<0.05) (Table 1).

One-way ANOVA showed significant between-group differences in the DTI metrics of WMH or normal white matter in six regions (p<0.001). FA, MD, and DR values of WMH in the pFH and pFLV showed no significant between-group differences; however, their observed values differed greatly from those of other regions. In WMHs with a Fazekas grade of 1, the FA values of the WMHs in the pFH (**0.24 ± 0.05**) and pFLV (**0.21 ± 0.04**) were significantly lower than those observed within the pOH (**0.46 ± 0.09**) (both p<0.001), pPLV (**0.49 ± 0.06**) (both p<0.001), dFCO (**0.47 ± 0.10**) (both p<0.001), and dPCO (**0.43 ± 0.07**) (both p<0.001).

Meanwhile, the MD values of WMHs in the pFH (**10.10 ± 0.81**) and the pFLV (**9.65 ± 0.80**) were significantly higher those that of the pOH (**8.03 ± 0.84**) (both p<0.001), pPLV (**6.59 ± 0.55**) (both p<0.001), dFCO (**7.07 ± 0.77**) (both p<0.001), and dPCO (**6.84 ± 0.60**) (both p<0.001). The DR values of WMHs in the pFH (**8.84 ± 0.88**) and pFLV (**8.62 ± 0.89**) were also significantly higher than those of the pOH (**5.86 ± 1.05**) (both p<0.001), pPLV (**4.66 ± 0.50**) (both p<0.001), dFCO (**5.19 ± 0.94)** (both p<0.001)**,** and dPCO (**5.21 ± 0.74**) (both p<0.001) . The DA values of WMHs in the pFH (**12.6 ± 0.92**) and pFLV (**11.68 ± 0.75**) were significantly higher than those of the pPLV (**10.44 ± 1.19**) (p<0.001 and p<0.05, respectively), dFCO (**10.85 ± 1.20**) (p<0.001 and p<0.05, respectively), and dPCO (**10.11 ± 0.79**) (both p<0.001) .

We observed similar differences in DTI metrics within the pFH, pFLV, and other regions that were Fazekas grades 2 and 3. However, differences between pFH, pFLV, and other regions were not so obvious in normal white matter. The FA values of normal pFH (0.61 ± 0.13) were significantly lower than those of pOH (0.75 ± 0.04) (p<0.001) and dFCO (0.78 ± 0.04) (p<0.001). The FA of normal pFLV (0.51 ± 0.10) was significantly lower than that of pOH (p<0.001), dFCO (p<0.001) and dPCO (0.67 ± 0.06) (p<0.001). Meanwhile, the MD values of normal pFH (5.13 ± 0.63) were significantly lower than those of dFCO (4.50 ± 0.28) (p<0.05). The MD of normal pFLV (5.83 ± 0.71) was significantly higher than that of pPLV (5.11 ± 0.40) (p<0.05), dFCO (4.50 ± 0.28) (p<0.001), and dPCO (4.89 ± 0.47) (p<0.001). The DA values of normal pFH (9.05 ± 0.90) were significantly lower than those of pOH (11.70 ± 1.15) (p<0.001), the DA value of the normal pFLV was significantly lower than that of pOH (p<0.001). The DR values of normal pFH (3.17 ± 0.95) were significantly higher than those of dFCO (1.96 ± 0.34) (p<0.001). The DR values of normal pFLV (4.08 ± 0.92) were significantly higher than those of pOH (2.59 ± 0.41) (p<0.001), pPLV (3.35 ± 0.53) (p<0.05), dFCO (1.96 ± 0.34) (p<0.001) and dPCO (2.98 ± 0.92) (p<0.001) (Tables 2–5).

Another interesting finding was that FA, MD, and DR values of WMHs from the pFH and pFLV changed dramatically from Fazekas grade 0 to 1, but not significantly from Fazekas grade 1 to 3. The WMHs of other regions changed gradually from Fazekas grades 0 to 3 (Figures 2–5).

Discussion

Pathological studies have revealed the histological heterogeneity and severities of WMH. These include myelin pallor, enlargement of perivascular spaces, discontinuity of ependyma, infarctions, gliosis, and axonal loss [13, 18-20]. Nevertheless, these pathologic changes induce similar signals via FLAIR or T2WI and are difficult to distinguish. Some studies have suggested that pathological differences exist between periventricular WMHs and deep WMHs [21-24]. Our results demonstrated that microstructural changes around the frontal periventricular WMHs were significantly different from those in other regions, Meanwhile, the structural changes within parietal-occipital periventricular WMHs resembled those of deep white matter.

There were significantly lower FA values, but higher DA, DR, and MD values in frontal periventricular WMHs compared to other regions. These results underscore the pathological heterogeneity of WMHs in different regions. Studies with magnetization transfer imaging also showed a lower magnetization transfer ratio in frontal periventricular WMHs compared to parieto-occipital periventricular WMHs [16, 17]. As there were no such differences in DTI metrics among different brain regions that featured normal white matter. Therefore, these heterogeneities were likely not due to anatomical heterogeneities.

Frontal periventricular WMHs might correspond with more severe pathological processes than other regions. Frontal WMHs appeared at an earlier age and demonstrated less age-related progression than WMHs in other regions [14]. This may lead to inconsistencies between the extent of WMHs and their respective pathological severities. The underlying pathological changes may be aggravated, even with little volumetric expansion. These findings suggest that future studies should consider, not only the volume of WMH, but also their pathological severities.

Previous studies have mostly assessed the relationship between volumetric measures of WMH and functional decline. Fazekas et al. [2] categorized periventricular WMHs into three grades. Moderate and severe (grades 2 and 3) periventricular WMHs were believed to be related to ischemia, whereas mild (grade 1) periventricular WMHs were considered non-ischemic, mainly due to a partial loss of the ependymal lining [3]. However, correlations between the volume of WMHs and cognitive performance were modest. Therefore, many clinical variations cannot be explained by volumetric measurements.

Some studies [4-6] have elucidated links between cognitive decline and periventricular WMHs in the frontal lobe, parieto-occipital lobe, and other parts of the brain. However, the underlying pathological mechanisms of WMHs in different regions that might explain cognitive decline (other than anatomical locations) remain scarcely studied [4].

Some pathological studies suggested that periventricular WMHs occurred because of fluid accumulation within the extracellular space that was related to the loss of ventricular ependyma [25-27]. Although increases in interstitial water content might have led to significant increases in MD, these changes could not explain the more immediate changes in DR values, compared to DA values. Thus, demyelination may have contributed to these pathological changes. Further, these changes may have led to rapid increases in DR and relatively mild changes in DA [28].

Immunohistochemical findings revealed that periventricular WMHs demonstrated more severe demyelination than deep WMHs [25]. A past neuropathological study found a stronger relationship between the extent of WMHs on MRI and the extent of myelin rarefaction in the frontal lobe, compared to the parietal lobe [29]. These findings suggested that even Fazekas grade 1 WMHs may correspond to clinically significant pathological changes around the frontal lateral ventricle. Frontal white matter microstructural changes began before the appearance of hyperintensities that could be found using conventional MRI.

A recent DTI study [5] showed that, in patients with hypertension, anterior thalamic radiations, the superior longitudinal fasciculus, and the forceps minor had significantly lower FA and significantly higher MD, AD, and RD values; these changes corresponded with measures of cognitive impairment. In Duering's study [7] of cerebral autosomal dominant

arteriopathy with subcortical infarcts and leukoencephalopathy (CADASIL), anterior thalamic radiations and frontal forceps were also considered key sites of cognitive impairment. These results suggested that frontal WMHs may contribute to functional impairments.

There were some limitations to our study. First, normal white matter FA values decreased with age, while MD values increased with age. Our control group was significantly younger, on average, than our patient group. However, the differences between WMHs and standard DTI metrics were greater than the normal variation observed with age [30]. Second, to minimize the influence of DTI parameters caused by anatomical variations, we selected ROIs within identical white matter tracts, according to the color maps; however, variations may still exist. Third, since the structural changes reflected by DTI parameters were non-specific and may have been affected by many factors, relevant pathological changes remain poorly elucidated.

Conclusions

Our results showed that pathological processes differed among frontal periventricular WMHs, parietal-occipital periventricular WMHs, and deep WMHs. These differences may be due to more severe demyelination in the frontal white matter tracts. Future studies should consider pathological heterogeneity as a factor to better explore the relationships between WMHs and cognitive impairment.

Abbreviations

WMHs: White matter hyperintensities T2WI: T2-weighted imaging FLAIR: fluid-attenuated inversion recovery MRI: magnetic resonance imaging DTI: Diffusion tensor imaging FA: fractional anisotropy MD: mean diffusivity (MD) DA:axial diffusivity DR: radial diffusivity ROIs: regions of interest (ROIs) pFH: periventricular white matter around the frontal horn pFLV: periventricular white matter around the frontal lateral ventricle pOH: periventricular white matter around the occipital horn pPLV: periventricular white matter around the parietal lateral ventricle dFCO: deep white matter of the frontal centrum ovale dPCO: deep white matter of the parietal centrum ovale CADASIL: cerebral autosomal dominant arteriopathy with subcortical infarcts and leukoencephalopathy (CADASIL)

Declarations

Ethics approval and consent to participate

The Institutional Review Board of Affiliated Yixing Hospital of Jiangsu University approved this study. Written informed consent for participation was obtained from the patient.

Consent to publication

Not applicable

Availability of data and materials

The datasets used and/or analysed during the current study are available from the supplementary material.

Competing interests

The authors declare that they have no competing interests.

Funding

This work was supported by the Foundation of Medical and Health Guiding Projects of Science and Technology Development in Wuxi City (No. 32). The foundation provided financial support for data pooling, analysis and writing of the manuscript.

Authors' contributions

ZM and HS performed statistical analysis, and were major contributor in writing the manuscript. LX, DY, XS and WX analyzed the clinical data and measured DTI metrics. HS and ZC assessed and grading WMH. ZC contributed to editing and revising the manuscript and supervised this publication. All authors read and approved the final manuscript.

Acknowledgements

Not applicable.

References

1. Bos D, Wolters FJ, Darweesh SKL, Vernooij MW, de Wolf F, Ikram MA, Hofman A: **Cerebral small vessel disease and the risk of dementia: A systematic review and meta-analysis of population-based evidence**. *Alzheimer's & dementia : the journal of the Alzheimer's Association* 2018, **14**(11):1482-1492.
2. Fazekas F, Chawluk JB, Alavi A, Hurtig HI, Zimmerman RA: **MR signal abnormalities at 1.5 T in Alzheimer's dementia and normal aging**. *AJR American journal of roentgenology* 1987, **149**(2):351-356.
3. Kim KW, MacFall JR, Payne ME: **Classification of white matter lesions on magnetic resonance imaging in elderly persons**. *Biological psychiatry* 2008, **64**(4):273-280.
4. Biesbroek JM, Weaver NA, Biessels GJ: **Lesion location and cognitive impact of cerebral small vessel disease**. *Clinical science (London, England : 1979)* 2017, **131**(8):715-728.
5. Carnevale L, D'Angelosante V, Landolfi A, Grillea G, Selvetella G, Storto M, Lembo G, Carnevale D: **Brain MRI fiber-tracking reveals white matter alterations in hypertensive patients without damage at conventional neuroimaging**. *Cardiovascular research* 2018, **114**(11):1536-1546.
6. Habes M, Sotiras A, Erus G, Toledo JB, Janowitz D, Wolk DA, Shou H, Bryan NR, Doshi J, Volzke H *et al*: **White matter lesions: Spatial heterogeneity, links to risk factors, cognition, genetics, and atrophy**. *Neurology* 2018.
7. Duering M, Zieren N, Herve D, Jouvent E, Reyes S, Peters N, Pachai C, Opherk C, Chabriat H, Dichgans M: **Strategic role of frontal white matter tracts in vascular cognitive impairment: a voxel-based lesion-symptom mapping study in CADASIL**. *Brain : a journal of neurology* 2011, **134**(Pt 8):2366-2375.
8. Cremers LG, de Groot M, Hofman A, Krestin GP, van der Lugt A, Niessen WJ, Vernooij MW, Ikram MA: **Altered tract-specific white matter microstructure is related to poorer cognitive performance: The Rotterdam Study**. *Neurobiology of aging* 2016, **39**:108-117.
9. Griffanti L, Jenkinson M, Suri S, Zsoldos E, Mahmood A, Filippini N, Sexton CE, Topiwala A, Allan C, Kivimaki M *et al*: **Classification and characterization of periventricular and deep white matter hyperintensities on MRI: A study in older adults**. *NeuroImage* 2018, **170**:174-181.
10. Bolandzadeh N, Davis JC, Tam R, Handy TC, Liu-Ambrose T: **The association between cognitive function and white matter lesion location in older adults: a systematic review**. *BMC neurology* 2012, **12**:126.
11. de Laat KF, van Norden AG, van Oudheusden LJ, van Uden IW, Norris DG, Zwiers MP, de Leeuw FE: **Diffusion tensor imaging and mild parkinsonian signs in cerebral small vessel disease**. *Neurobiology of aging* 2012, **33**(9):2106-2112.

12. van Norden AG, de Laat KF, van Dijk EJ, van Uden IW, van Oudheusden LJ, Gons RA, Norris DG, Zwiers MP, de Leeuw FE: **Diffusion tensor imaging and cognition in cerebral small vessel disease: the RUN DMC study**. *Biochimica et biophysica acta* 2012, **1822**(3):401-407.
13. Prins ND, Scheltens P: **White matter hyperintensities, cognitive impairment and dementia: an update**. *Nat Rev Neurol* 2015, **11**(3):157-165.
14. Habes M, Sotiras A, Erus G, Toledo JB, Janowitz D, Wolk DA, Shou H, Bryan NR, Doshi J, Volzke H *et al*: **White matter lesions: Spatial heterogeneity, links to risk factors, cognition, genetics, and atrophy**. *Neurology* 2018, **91**(10):e964-e975.
15. van Leijsen EMC, Bergkamp MI, van Uden IWM, Ghafoorian M, van der Holst HM, Norris DG, Platel B, Tuladhar AM, de Leeuw FE: **Progression of White Matter Hyperintensities Preceded by Heterogeneous Decline of Microstructural Integrity**. *Stroke; a journal of cerebral circulation* 2018, **49**(6):1386-1393.
16. Spilt A, Goekoop R, Westendorp RG, Blauw GJ, de Craen AJ, van Buchem MA: **Not all age-related white matter hyperintensities are the same: a magnetization transfer imaging study**. *AJNR American journal of neuroradiology* 2006, **27**(9):1964-1968.
17. Bastin ME, Clayden JD, Pattie A, Gerrish IF, Wardlaw JM, Deary IJ: **Diffusion tensor and magnetization transfer MRI measurements of periventricular white matter hyperintensities in old age**. *Neurobiology of aging* 2009, **30**(1):125-136.
18. Gouw AA, Seewann A, van der Flier WM, Barkhof F, Rozemuller AM, Scheltens P, Geurts JJ: **Heterogeneity of small vessel disease: a systematic review of MRI and histopathology correlations**. *Journal of neurology, neurosurgery, and psychiatry* 2011, **82**(2):126-135.
19. Haller S, Kovari E, Herrmann FR, Cuvinciuc V, Tomm AM, Zulian GB, Lovblad KO, Giannakopoulos P, Bouras C: **Do brain T2/FLAIR white matter hyperintensities correspond to myelin loss in normal aging? A radiologic-neuropathologic correlation study**. *Acta neuropathologica communications* 2013, **1**:14.
20. Lin J, Wang D, Lan L, Fan Y: **Multiple Factors Involved in the Pathogenesis of White Matter Lesions**. *BioMed research international* 2017, **2017**:9372050.
21. Valdes Hernandez MC, Piper RJ, Bastin ME, Royle NA, Maniega SM, Aribisala BS, Murray C, Deary IJ, Wardlaw JM: **Morphologic, distributional, volumetric, and intensity characterization of periventricular hyperintensities**. *AJNR American journal of neuroradiology* 2014, **35**(1):55-62.
22. Anderson VC, Obayashi JT, Kaye JA, Quinn JF, Berryhill P, Riccelli LP, Peterson D, Rooney WD: **Longitudinal relaxographic imaging of white matter hyperintensities in the elderly**. *Fluids and barriers of the CNS* 2014, **11**:24.
23. Murray ME, Vemuri P, Preboske GM, Murphy MC, Schweitzer KJ, Parisi JE, Jack CR, Jr., Dickson DW: **A quantitative postmortem MRI design sensitive to white matter hyperintensity differences and their relationship with underlying pathology**. *Journal of neuropathology and experimental neurology* 2012, **71**(12):1113-1122.
24. Stenset V, Hofoss D, Berstad AE, Negaard A, Gjerstad L, Fladby T: **White matter lesion subtypes and cognitive deficits in patients with memory impairment**. *Dementia and geriatric cognitive disorders* 2008, **26**(5):424-431.
25. Simpson JE, Fernando MS, Clark L, Ince PG, Matthews F, Forster G, O'Brien JT, Barber R, Kalaria RN, Brayne C *et al*: **White matter lesions in an unselected cohort of the elderly: astrocytic, microglial and oligodendrocyte precursor cell responses**. *Neuropathology and applied neurobiology* 2007, **33**(4):410-419.
26. O'Sullivan M: **Leukoaraiosis**. *Practical neurology* 2008, **8**(1):26-38.
27. Fernando MS, Simpson JE, Matthews F, Brayne C, Lewis CE, Barber R, Kalaria RN, Forster G, Esteves F, Wharton SB *et al*: **White matter lesions in an unselected cohort of the elderly: molecular pathology suggests origin from chronic hypoperfusion injury**. *Stroke; a journal of cerebral circulation* 2006, **37**(6):1391-1398.

28. Abhinav K, Yeh FC, Pathak S, Suski V, Lacomis D, Friedlander RM, Fernandez-Miranda JC: **Advanced diffusion MRI fiber tracking in neurosurgical and neurodegenerative disorders and neuroanatomical studies: A review**. *Biochimica et biophysica acta* 2014, **1842**(11):2286-2297.
29. Smith CD, Snowdon D, Markesbery WR: **Periventricular white matter hyperintensities on MRI: correlation with neuropathologic findings**. *Journal of neuroimaging : official journal of the American Society of Neuroimaging* 2000, **10**(1):13-16.
30. Abe O, Aoki S, Hayashi N, Yamada H, Kunimatsu A, Mori H, Yoshikawa T, Okubo T, Ohtomo K: **Normal aging in the central nervous system: quantitative MR diffusion-tensor analysis**. *Neurobiology of aging* 2002, **23**(3):433-441.

Tables

Table 1

Correlation coefficient between DTI metrics and Fazekas scale in different regions

	pFH	pFLV	pOH	pPLV	dFCO	dPCO
FA	-0.508	-0.513	-0.648	-0.417*	-0.781	-0.825
MD	0.777	0.819	0.823	0.861	0.835	0.899
DA	0.806	0.840	0.749	0.831	0.545	0.675
DR	0.733	0.781	0.768	0.756	0.844	0.897

***P<0.05, The other P-values were all < 0.001.** pFH: periventricular white matter around the frontal horn; pFLV: periventricular white matter around the frontal lateral ventricle; pOH: periventricular white matter around the occipital horn; pPLV: periventricular white matter around the parietal lateral ventricle; dFCO: deep white matter of the frontal centrum ovale; dPCO: deep white matter of the parietal centrum ovale.

Table 2

Comparison of FA values in different regions with the same Fazekas scale

	pFH	pFLV	pOH	pPLV	dFCO	dPCO	F/P value
0	0.61±0.13$^{\#\S\dagger}$	0.51±0.10$^{\#\ddagger i\int}$	0.75±0.04$^{\S\ddagger\blacktriangle *}$	0.59±0.08$^{\blacktriangle\blacktriangledown}$	0.78±0.04$^{\dagger i\blacktriangledown\Delta}$	0.67±0.06 $^{\int *\Delta}$	26.578/P<0.001
1	0.24±0.05$^{\S\dagger\ddagger i}$	0.21±0.04$^{\int\blacktriangle\blacktriangledown\P}$	0.46±0.09$^{\S\int}$	0.49±0.06$^{\dagger\blacktriangle}$	0.47±0.10$^{\ddagger\blacktriangledown}$	0.43±0.07$^{i\ \P}$	84.728/P<0.001
2	0.25±0.04$^{\S\dagger\ddagger i}$	0.22±0.02$^{\int\blacktriangle\blacktriangledown\P}$	0.48±0.07$^{\S\int\#}$	0.46±0.10$^{\dagger\blacktriangle *}$	0.43±0.10$^{\ddagger\blacktriangledown}$	0.38±0.07$^{i\ \P\#*}$	44.705/P<0.001
3	0.23±0.05$^{\S\dagger\ddagger i}$	0.20±0.05$^{\int\blacktriangle\blacktriangledown\P}$	0.43±0.07$^{\S\int\#\blacklozenge}$	0.47±0.10$^{\dagger\blacktriangle\heartsuit\bullet}$	0.35±0.05$^{\ddagger\blacktriangledown\#\heartsuit\clubsuit}$	0.33±0.05$^{i\ \P\blacklozenge\bullet\clubsuit}$	44.923/P<0.001

P<0.05 # * Δ◊□● ; P<0.001§† ‡ i ∫ ▲▼¶♦♥●♣. pFH: periventricular white matter around the frontal horn; pFLV: periventricular white matter around the frontal lateral ventricle; pOH: periventricular white matter around the occipital horn; pPLV: periventricular white matter around the parietal lateral ventricle; dFCO: deep white matter of the frontal centrum ovale; dPCO: deep white matter of the parietal centrum ovale.

Table 3

Comparison of MD values(mm^2s^{-1}) in different regions with the same Fazekas scale

	pFH	pFLV	pOH	pPLV	dFCO	dPCO	F/P value
0	5.13±0.63#*	5.83±0.71#Δ§†	5.62±0.48◊‡□	5.11±0.40Δ◊●	4.50±0.28*§‡●	4.89±0.47†□	15.793/P<0.001
1	10.10±0.81§†‡i	9.65±0.80∫▲▼¶	8.03±0.84§∫♦#*	6.59±0.55†▲♦	7.07±0.77‡▼#	6.84±0.60i ¶*	84.325/P<0.001
2	10.90±0.86§†‡i	10.72±0.77∫▲▼¶	8.25±0.96§∫#	7.13±1.05†▲#	7.60±0.43‡▼	7.59±0.40i ¶	68.275/P<0.001
3	11.75±1.10§†‡i	11.22±0.93∫▲▼¶	9.81±1.00§∫♦♥●	8.28±6.80†▲♦	8.36±0.72‡▼♥	8.58±0.89i ¶●	46.955/P<0.001

P<0.05 # * Δ◊□●, P<0.001 §† ‡ i ∫ ▲▼¶♦♥●♣. pFH: periventricular white matter around the frontal horn; pFLV: periventricular white matter around the frontal lateral ventricle; pOH: periventricular white matter around the occipital horn; pPLV: periventricular white matter around the parietal lateral ventricle; dFCO: deep white matter of the frontal centrum ovale; dPCO: deep white matter of the parietal centrum ovale.

Table 4

Comparison of DA values(mm^2s^{-1}) in different regions with the same Fazekas scale

	pFH	pFLV	pOH	pPLV	dFCO	dPCO	F/P value
0	9.05±0.90§	9.38±1.10†	11.70±1.15§†‡ i ∫	8.63±0.84‡#	9.58±0.60 i #	9.24±1.15 ∫	21.923/P<0.001
1	12.6±0.92#§†‡	11.68±0.75#*Δi	12.37±1.12∫▲▼	10.44±1.19§*∫	10.85±1.20†Δ▲	10.11±0.79‡i▼	20.558/P<0.001
2	13.80±0.98§†‡	13.17±0.95i #∫	12.96±1.03▲*Δ	10.92±1.41§i ▲	11.46±1.41†#*	11.08±1.06‡∫Δ	17.846/P<0.001
3	14.59±1.18#§†	13.61±0.99*‡i	14.76±0.91*∫▲▼	12.96±1.32#∫Δ◊	11.60±1.31§‡▲Δ	11.63±1.20†i▼◊	26.301/P<0.001

P<0.05 # * Δ◊▯●, P<0.001 §† ‡ i ∫ ▲▼¶♦♥●♣. pFH: periventricular white matter around the frontal horn; pFLV: periventricular white matter around the frontal lateral ventricle; pOH: periventricular white matter around the occipital horn; pPLV: periventricular white matter around the parietal lateral ventricle; dFCO: deep white matter of the frontal centrum ovale; dPCO: deep white matter of the parietal centrum ovale.

Table 5

Comparison of DR values(mm^2s^{-1}) in different regions with the same Fazekas scale

	pFH	pFLV	pOH	pPLV	dFCO	dPCO	F/P value
0	3.17±0.95$^{\#\S}$	4.08±0.92$^{\#\dagger *\ddagger i}$	2.59±0.41$^{\dagger\Delta\diamond}$	3.35±0.53$^{*\Delta\int▯}$	1.96±0.34$^{\S\ddagger\diamond\int●}$	2.98±0.92$^{i\ ▯●}$	23.077/P<0.001
1	8.84±0.88$^{\S\dagger\ddagger i}$	8.62±0.89$^{\int▲▼¶}$	5.86±1.05$^{\S\int\#}$	4.66±0.50$^{\dagger▲\#}$	5.19±0.94$^{\ddagger▼}$	5.21±0.74$^{i\ ¶}$	102.127/P<0.001
2	9.44±0.93$^{\S\dagger\ddagger i}$	9.49±0.74$^{\int▲▼¶}$	5.89±1.07$^{\S\int}$	5.23±1.16$^{\dagger▲}$	5.63±0.62$^{\ddagger▼}$	6.04±0.70$^{i\ ¶}$	79.339/P<0.001
3	10.33±1.17$^{\S\dagger\ddagger i}$	10.02±1.02$^{\int▲▼¶}$	7.33±1.18$^{\S\int♦}$	5.88±1.00$^{\dagger▲♦\#}$	6.74±0.56$^{\ddagger▼}$	7.05±0.89$^{i\ ¶\#}$	54.705/P<0.001

P<0.05 # * Δ◊▯●, P<0.001 §† ‡ i ∫ ▲▼¶♦♥●♣. pFH: periventricular white matter

Figures

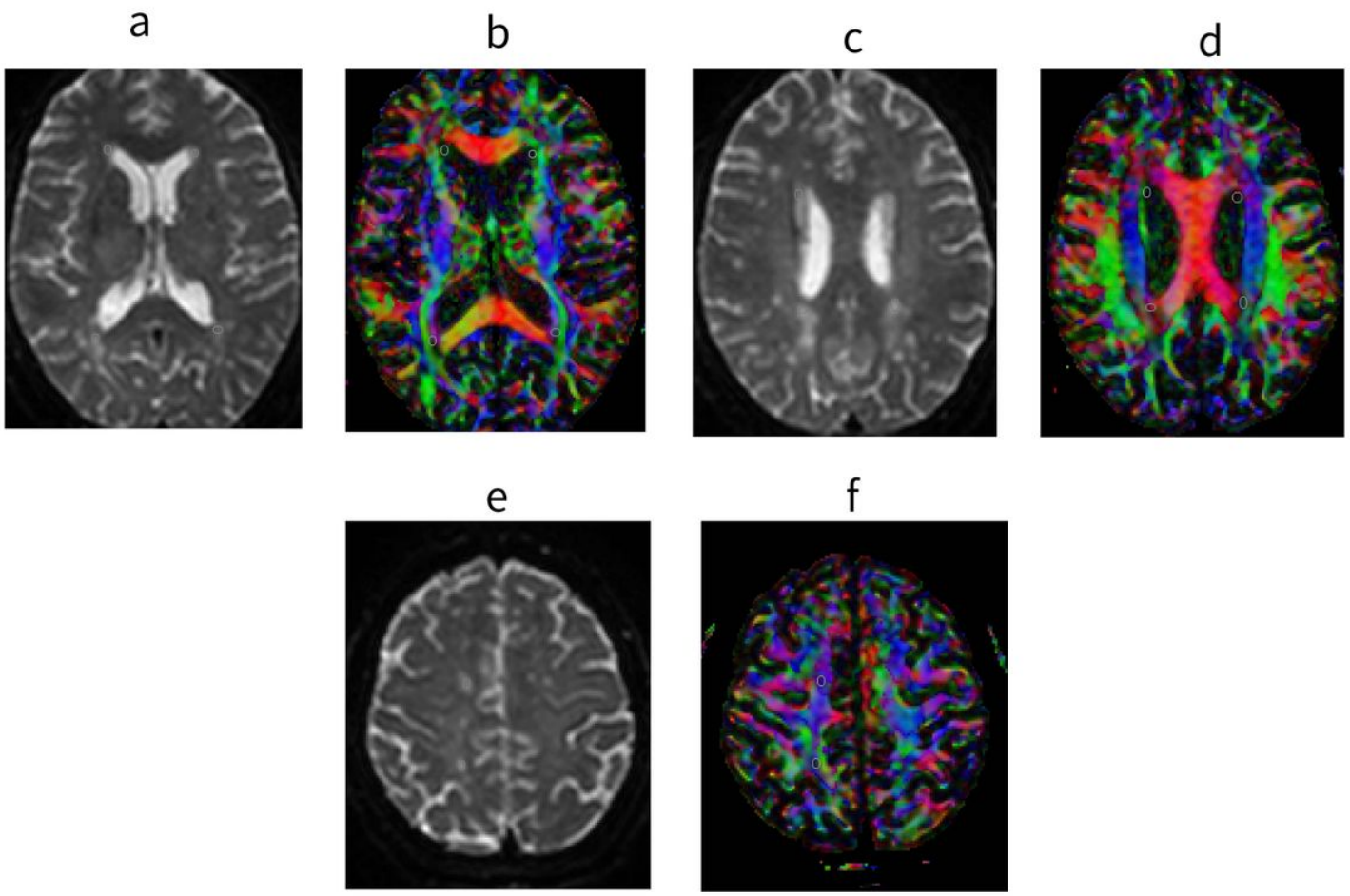

Figure 1

The region of interest (ROI) is determined on the B0 image (1a, 1c, 1e), and the corresponding colored FA maps (1b, 1d, 1f) is used to observe whether the ROI is located in the same white matter bundle. ROI around the frontal horn (pFH) were located in the anterior thalamic radiation, ROI around the occipital horn (pOH) were located in the tapetum and the posterior region of corona radiata, ROI around the frontal lateral ventricle (pFLV) were located in the superior fronto-occipital fasciculus, ROI around the parietal lateral ventricle (pPLV) were located in the junction of corpus callosum and parietal superior region of internal capsule, Two ROIs of deep white matter were located in the centrum ovale of frontal lobe (dFCO) and parietal lobe (dFCO) respectively.

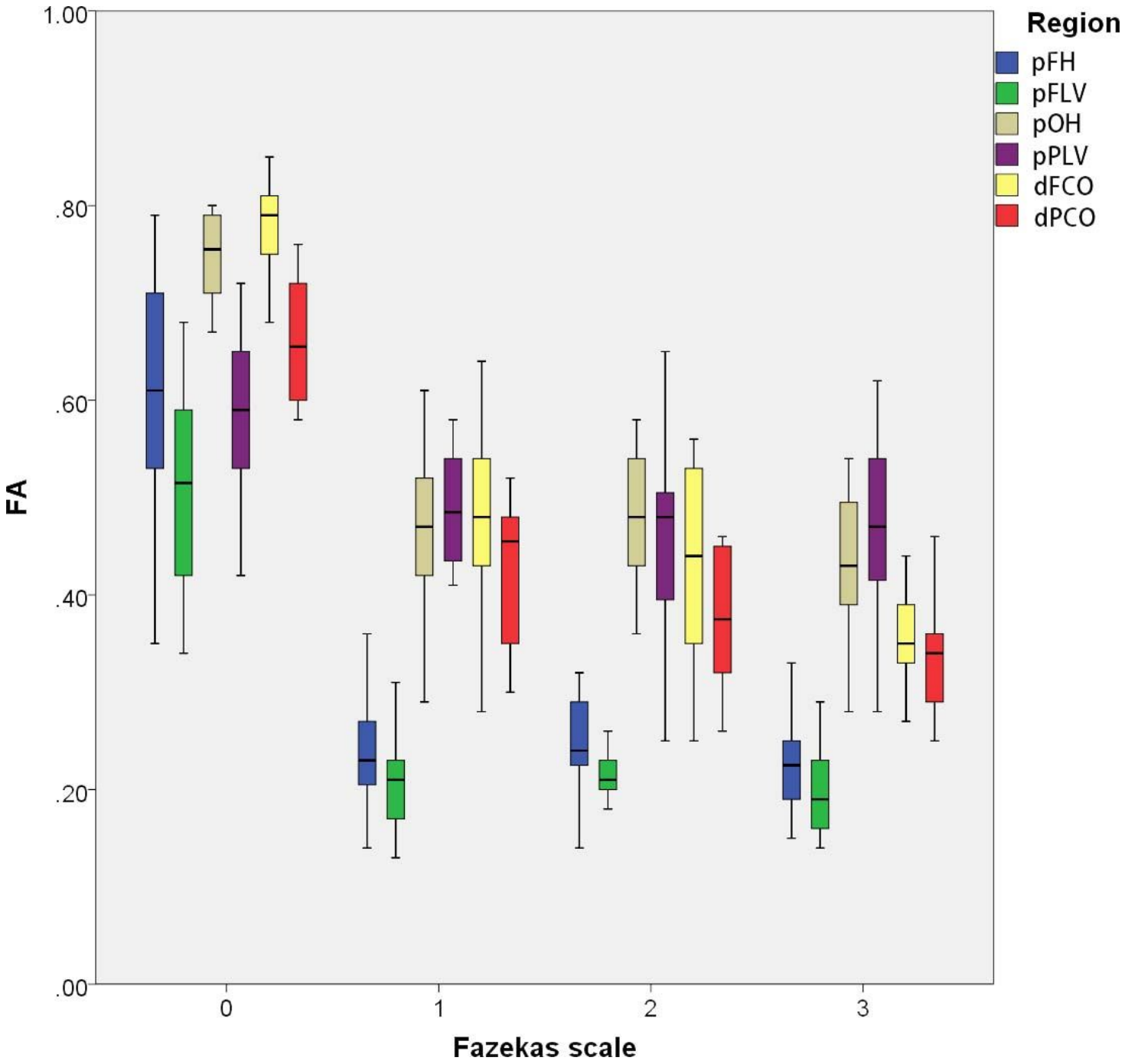

Figure 2

Progress of FA with Fazekas scale in different regions.

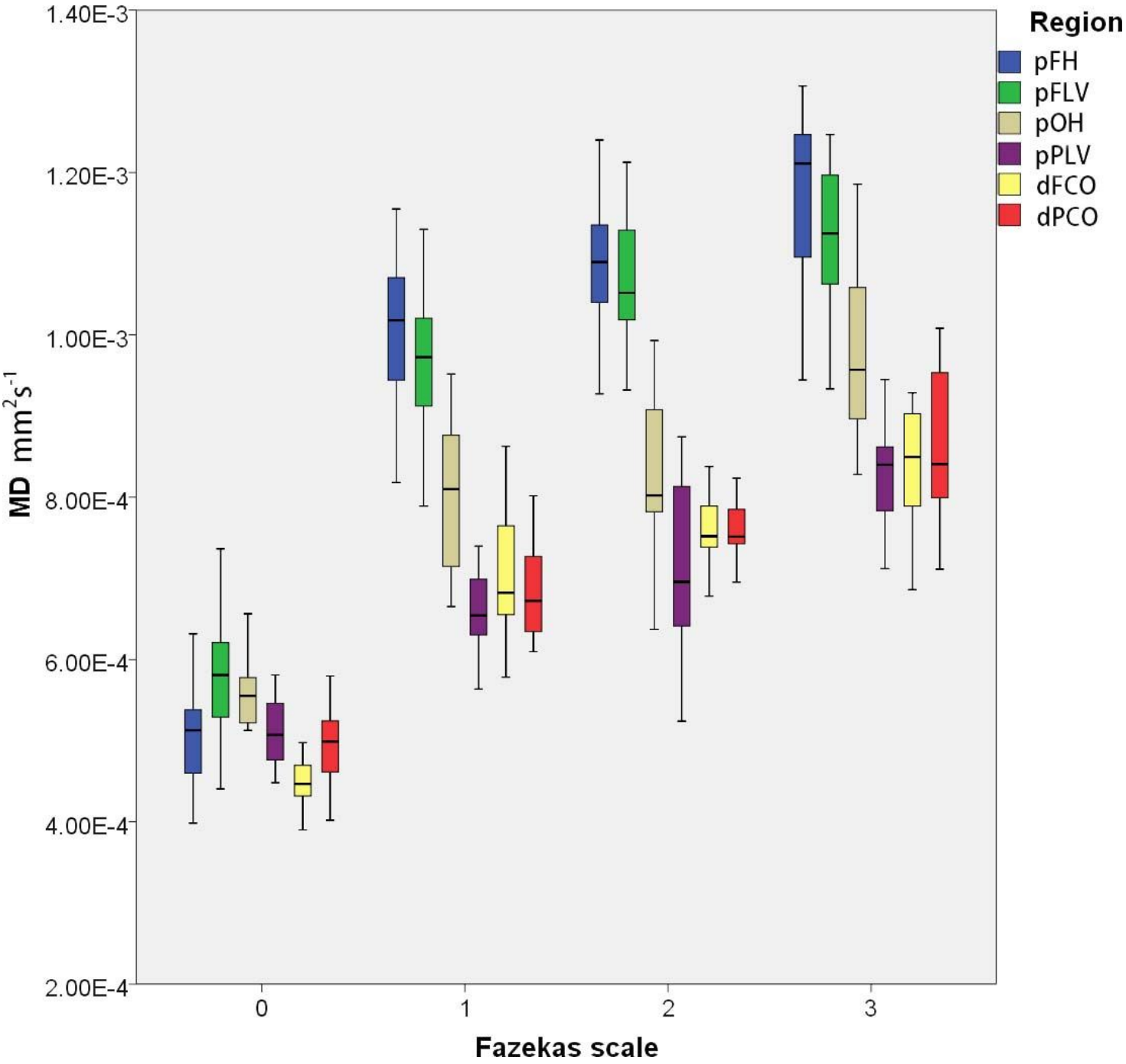

Figure 3

Progress of MD with Fazekas scale in different regions.

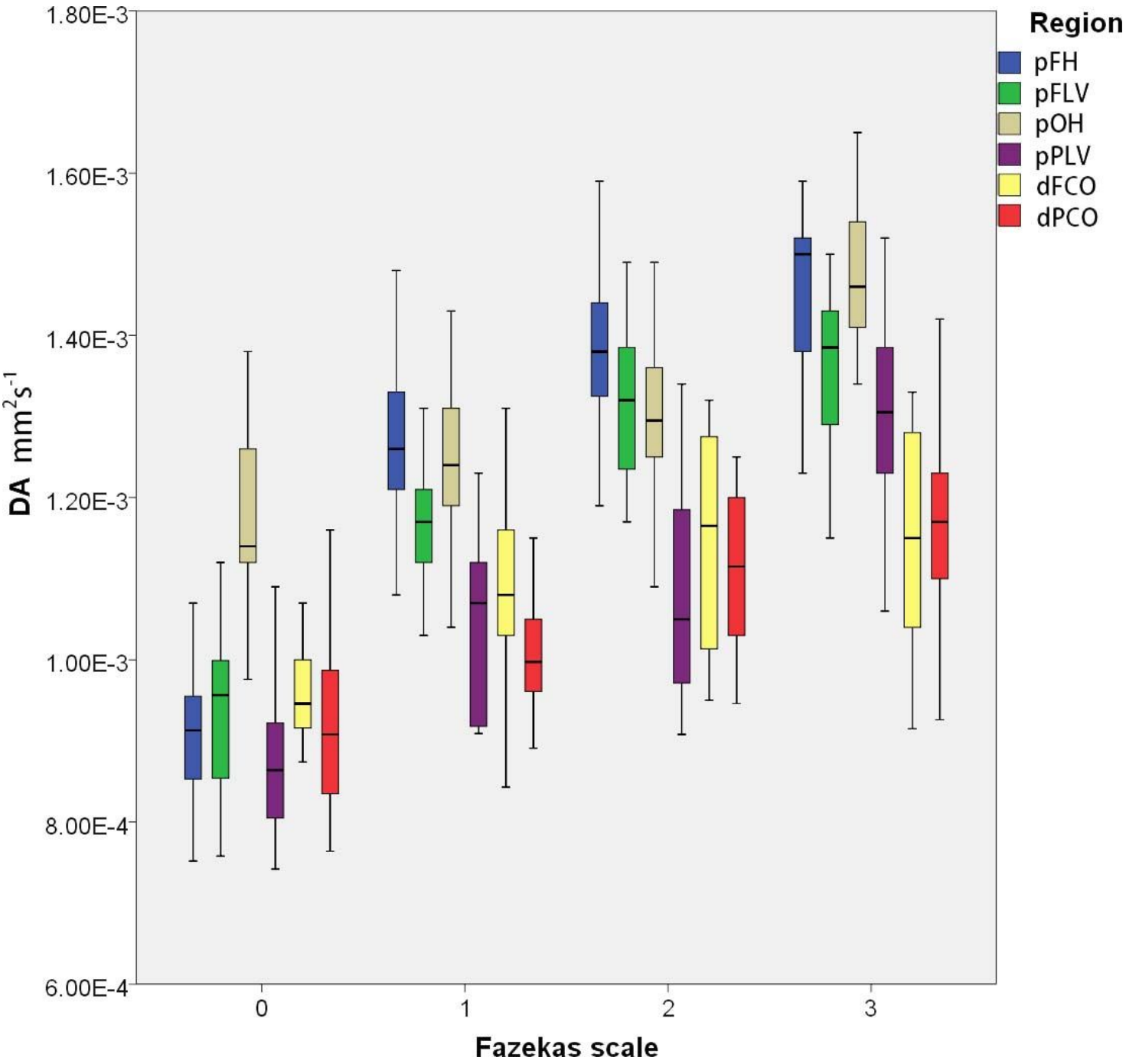

Figure 4

Progress of DA with Fazekas scale in different regions.

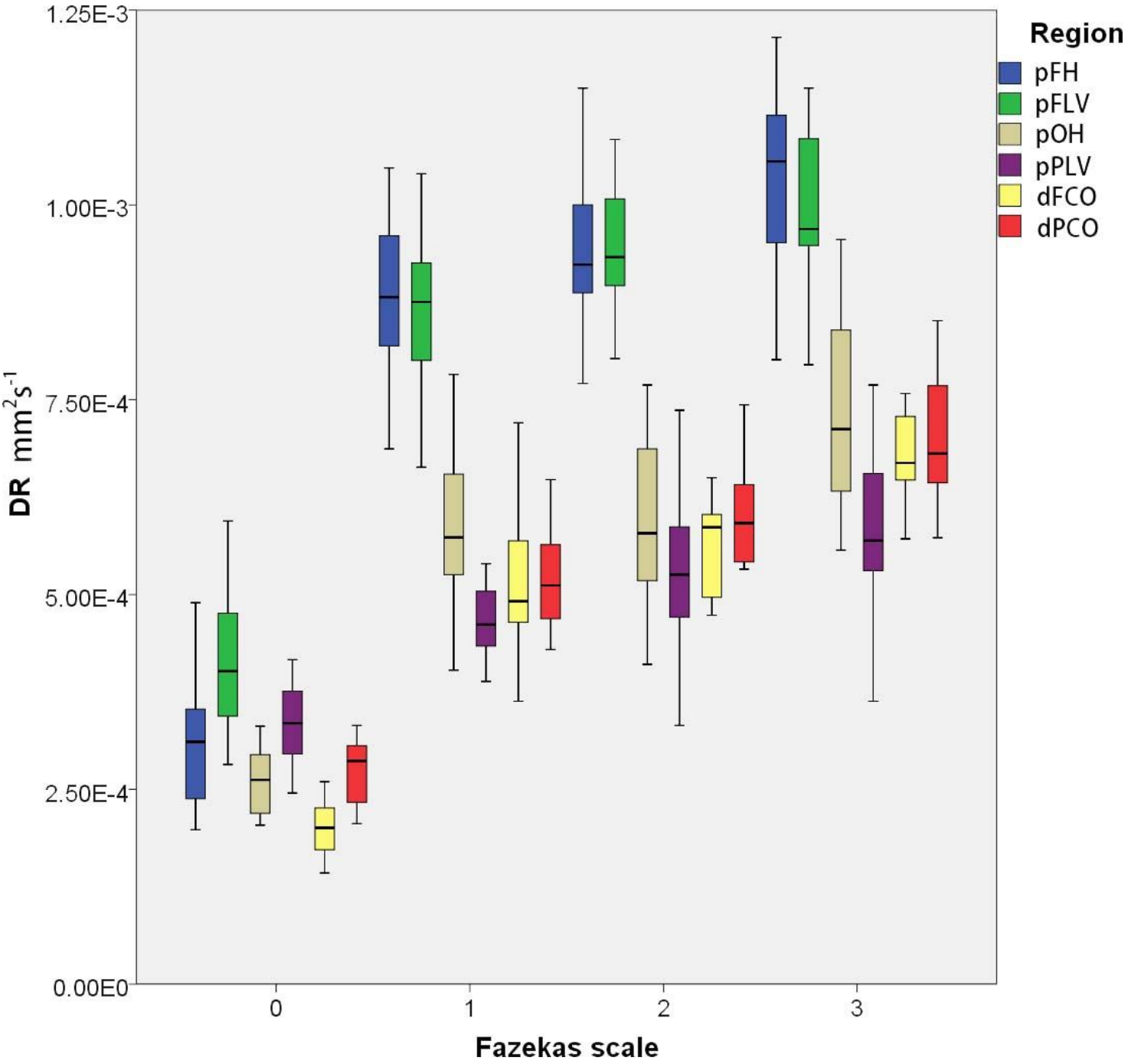

Figure 5

Progress of DR with Fazekas scale in different regions.

Supplementary Files

This is a list of supplementary files associated with this preprint. Click to download.

- Rawdata.xlsx